Weld World (2015) 59:785–796
DOI 10.1007/s40194-015-0252-1

RESEARCH PAPER

A study on the development of creep rupture and temper embrittlement properties in $2^1/_4$Cr-1Mo-V steel weld metal

G. Taniguchi[1] · K. Yamashita[1] · M. Otsu[1] · H. Nako[1] · M. Sakata[1,2]

Received: 9 February 2015 / Accepted: 16 June 2015 / Published online: 10 July 2015

Abstract $2^1/_4$Cr-1Mo-V steel, such as the ASTM A542/A542M type D, which has remarkable anti-hydrogen embrittlement and creep rupture properties, is widely used in main components such as pressure vessels in oil refinery plants. Submerged arc welding (SAW), shielded metal arc welding (SMAW), and gas-shielded tungsten arc welding (GTAW) consumables, equivalent to base metal, are selected for the welding of this steel. As referred to in American Society of Mechanical Engineers (ASME) Section VIII, various properties, such as tensile strength and impact toughness in addition to creep rupture, are required in $2^1/_4$Cr-1Mo-V steel weld metal. Especially in creep rupture properties, the lower limit of the design temperature, which is required in main components (mentioned above), was lowered from 470 to 440 °C, based on the revision of the ASME code in 2009. Additionally, temper embrittlement behavior, occurring under high temperature over a long period of time, should be considered as well when dealing with this deposited metal. In this study, we have discussed the validity of precipitates in order to develop the creep rupture and temper embrittlement properties of $2^1/_4$Cr-1Mo-V steel weld metal. As a result, it was found that MX in crystal grains improves creep rupture lifetime and that, in the prior γ grain boundaries, it inhibits embrittlement caused by the segration of impurities.

Keywords (IIW Thesaurus) Steels · Weld metal · Creep strength · Embrittlement · Segration · Impurities

Doc. IIW-2565, recommended for publication by Commission IX "Behaviour of Metals Subjected to Welding."

✉ G. Taniguchi
taniguchi.genichi@kobelco.com

K. Yamashita
yamashita.ken@kobelco.com

M. Otsu
otsu.minoru@kobelco.com

H. Nako
nako.hidenori@kobelco.com

[1] Kobe Steel, Ltd., 100-1, Miyamae, Fujisawa, Kanagawa 251-8551, Japan

[2] JGC Corporation, 2-3-1, Minato Mirai, Nishi-ku, Yokohama, Kanagawa 220-6001, Japan

1 Introduction

$2^1/_4$Cr-1Mo-V steel is widely used in main components such as pressure vessels in oil refinery plants, due to its remarkable anti-hydrogen embrittlement and creep rupture properties [1, 2]. The American Society of Mechanical Engineers (ASME) code and the American Petroleum Institute (API) recommended practice, which deal with the design and construction procedures of welded structures, are trying to establish optimal way for applying this comparably new steel. In the case of $2^1/_4$Cr-1Mo-V steel weld metal, ASME Section VIII Division 2 [3] regulates its principal chemical composition and creep rupture property, and API RP 934-A [4] deals with the limits of impurity level and temper embrittlement property, respectively.

In 2009, the revision of the ASME code required practically all $2^1/_4$Cr-1Mo-V steel reactors to contain certain creep rupture property. This steel weld metal also requires to meet the creep rupture property requirement specified in ASME Section VIII Division 2. The strength of low-alloy heat resistance steel, such as $2^1/_4$Cr-1Mo-V steel, at elevated temperatures is greatly affected by precipitates, such as carbonitride. Therefore, it is important to control the amount and shape of the precipitate to improve the creep rupture property of

Table 1 Chemical composition requirements of ASME Section VIII Division 2 for $2^1/_4$Cr-1Mo-V steel weld metal

Welding process	SAW	SMAW	GTAW	GMAW
C	0.05–0.15	0.05–0.15	0.05–0.15	0.05–0.15
Si	0.05–0.35	0.20–0.50	0.05–0.35	0.20–0.50
Mn	0.50–1.30	0.50–1.30	0.30–1.10	0.30–1.10
P	0.015 max.	0.015 max.	0.015 max.	0.015 max.
S	0.015 max.	0.015 max.	0.015 max.	0.015 max.
Cr	2.00–2.60	2.00–2.60	2.00–2.60	2.00–2.60
Mo	0.90–1.20	0.90–1.20	0.90–1.20	0.90–1.20
V	0.20–0.40	0.20–0.40	0.20–0.40	0.20–0.40
Nb	0.010–0.040	0.010–0.040	0.010–0.040	0.010–0.040

Unit /mass%

Max, maximum

the $2^1/_4$Cr-1Mo-V steel weld metal. However, the chemical composition of $2^1/_4$Cr-1Mo-V steel weld metal is specified by ASME Section VIII Division 2 as shown in Table 1. Therefore, its optimization is required within the limits of the ASME code so as to improve creep rupture property without degrading other mechanical properties, such as impact toughness and temper embrittlement.

On the other hand, specified limit of impurity level can be expressed as X-bar [5]: $(10P+5Sb+4Sn+As)\times10^{-2}$/ppm as referred in API RP 934-A and J-Factor [6]: $(Si+Mn)(P+Sn)\times10^4$, become more and more strict for inhibiting the temper embrittlement of material. However, in an industrial practice, it is more difficult to reduce the amount of impurities in the above than in the material currently used. Therefore, it is important to establish the material design, which inhibits temper embrittlement resulting from impurities. As shown in Fig. 1, it is commonly said that the temper embrittlement of Cr-Mo steel is caused by the segregation of impurity to the prior γ grain boundary during the tempering process [7]. In particular, the segregation of P to the prior γ grain boundary greatly degrades its bounding energy and hence, the effects of alloying elements to P segregation were evaluated [8]. However, the interaction between the precipitates and impurities in the prior γ grain boundary is not obvious though precipitates also exist together with impurities.

Therefore, the objective of the present investigation is to develop creep and temper embrittlement resistance of $2^1/_4$Cr-1Mo-V steel weld metal by modifying the morphology and types of the precipitates.

2 Experimental procedures

2.1 Materials

2.1.1 Materials for creep rupture test

Submerged arc welding (SAW) metal for the creep rupture test was prepared by the combination of solid-wire (diameter 4.0 mm) and sintered flux (mesh size 10×48). Figure 2 shows the welding groove configuration and pass sequences for SAW. ASME SA542 type D plates were used for the test. Table 2 shows the welding condition for SAW. Table 3 shows a typical chemical composition of tested SAW metal. The C, Cr, and Nb contents of SAW metal were controlled as 0.08–

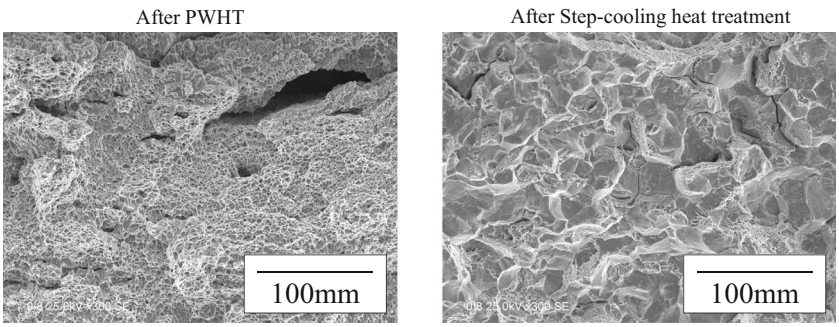

Fig. 1 Typical fractograph of Charpy V-notch specimen of $2^1/_4$Cr-1Mo-V steel weld metal

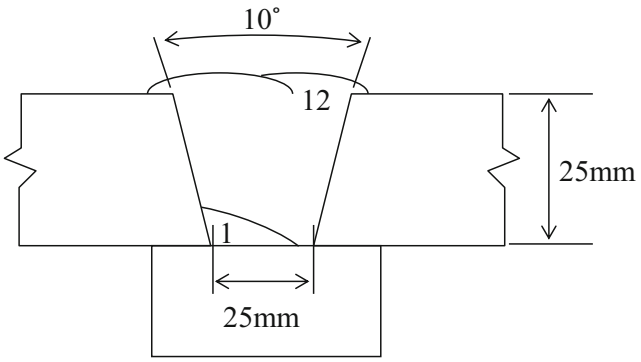

Fig. 2 Welding groove configuration and pass sequences for SAW

Table 2 Welding conditions for SAW (tandem)

Polarity	Welding current	Arc voltage	Travel speed	Heat input	Pass sequences
L: AC	L: 580 A	L: 30 V	60 cpm	36.0 kJ/cm	6 layers
T: AC	T: 580 A	T: 32 V			12 passes

Welding position, flat; preheat and interpass temperature, 200–250 °C

Table 3 Chemical compositions of SAW metal

C	Si	Mn	P	S	Cr	Mo	V	Nb
0.08	0.20	1.10	0.006	0.003	2.45	1.00	0.35	0.015

Unit /mass%; J-Factor =75; X-bar =7 ppm

0.12 mass%C, 2.1–2.8 mass%Cr, and non-addition to 0.08 mass%Nb, respectively.

2.1.2 Materials for the temper embrittlement test

Shielded metal arc welding (SMAW) metal for temper embrittlement test was prepared by a covered electrode (diameter of core rod 5.0 mm). Figure 3 shows the welding groove configuration and pass sequences for SMAW. ASME SA542 type D plates were used for the test. Table 4 shows the welding condition for SMAW.

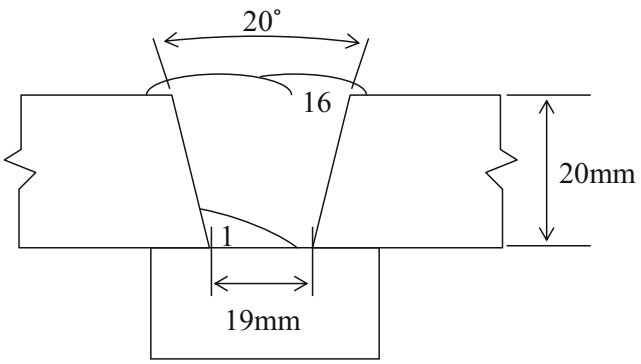

Fig. 3 Welding groove configuration and pass sequences for SMAW

Table 4 Welding conditions for SMAW

Polarity	Welding current	Arc voltage	Travel speed	Heat input	Pass sequence
AC	215 A	25 V	10–15 cpm	25–30 kJ/cm	8 layers 16 passes

Welding position, flat; preheat and interpass temperature, 200–250 °C

Table 5 Chemical composition of SMAW metal

C	Si	Mn	P	S	Cr	Mo	V	Nb
0.08	0.32	1.00	0.006	0.001	2.39	1.05	0.32	0.022

Unit, /mass%; J-Factor =132, X-bar =9 ppm

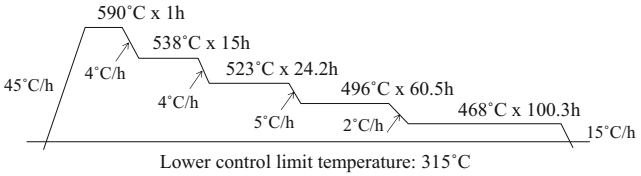

Fig. 4 Step cooling heat treatment (Socal No.1 type)

Chemical composition of each SMAW metal satisfies the ASME Section VIII Division 2 as referred to in Table 1. Table 5 shows a typical chemical composition of SMAW metal. The C, Mn, Cr, Mo, V, and Nb contents of SMAW metal were controlled as 0.08–0.11 mass%C, 0.7–1.0 mass%Mn, 2.2–2.7 mass%Cr, 0.9–1.1 mass%Mo, 0.25–0.40 mass%V, and 0.01–0.03 mass%Nb, respectively.

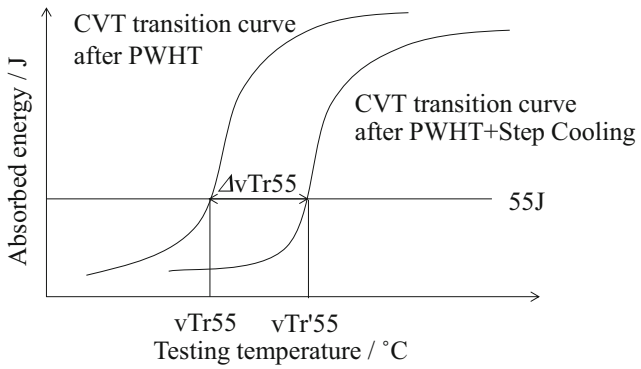

Fig. 5 Schematic for defining ΔvTr55

Table 6 Creep deformation of material identified by stress component (n) in Eq. 1

Creep deformation	Stress component (n)
Dislocation creep	≥3
Grain boundary sliding	2
Diffusion creep (grain boundary diffusion, lattice creep)	1

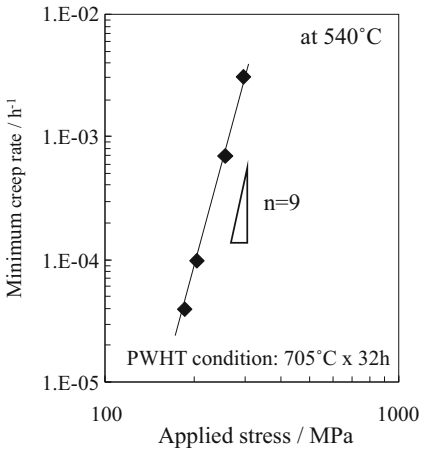

Fig. 6 Relationship between applied stress and creep rate at 540 °C of $2^1/_4$Cr-1Mo-V steel SAW metal

2.2 PWHT conditions

SMAW and SAW metals were subjected to post-weld heat treatment (PWHT) of 705 °C × 8 h for the Charpy V-notch test (CVT) and 705 °C × 32 h for the creep rupture test, respectively. The lower control limit for the PWHT temperature was 300 °C, while both the heating and cooling rates above the lower control limit temperature were 55 °C/h or lower.

In addition, the subset of SMAW metal was subjected to step cooling heat treatment (Socal No.1 type) as shown in Fig. 4 after PWHT so as to evaluate temper embrittlement sensitivity.

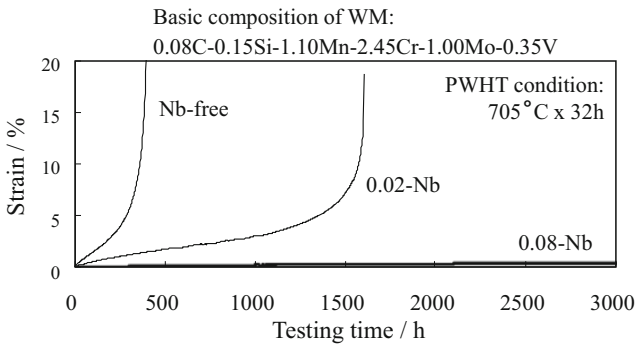

Fig. 7 Creep curves of Nb-controlled $2^1/_4$Cr-1Mo-V steel SAW metal

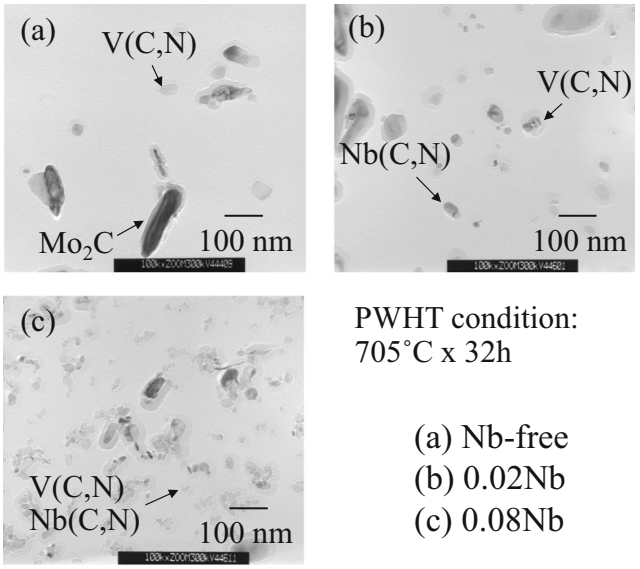

Fig. 8 TEM images of Nb-controlled $2^1/_4$Cr-1Mo-V steel SAW metal

2.3 Mechanical properties evaluation of weld metal

Both the creep rupture test and CVT specimen were extracted from the cross section of the test plate and the center of the deposited metal and 1/2 t position of the test plate.

The diameter of parallel part and gauge length of the creep rupture test specimen was 13/52 mm (4D). The creep rupture test was basically conducted with a testing temperature of 540 °C and 210 MPa of applied stress as referred to in the ASME code.

The CVT specimen had a 2-mm V-notch according to the American Welding Society (AWS) B4.0. The CVT was conducted according to the AWS A5.5 for the SMAW metal and A5.23 for the SAW metal, and test temperature to evaluate impact toughness was −30 °C. Temper embrittlement sensitivity was defined as the shift amount of vTr55 (=ΔvTr55),

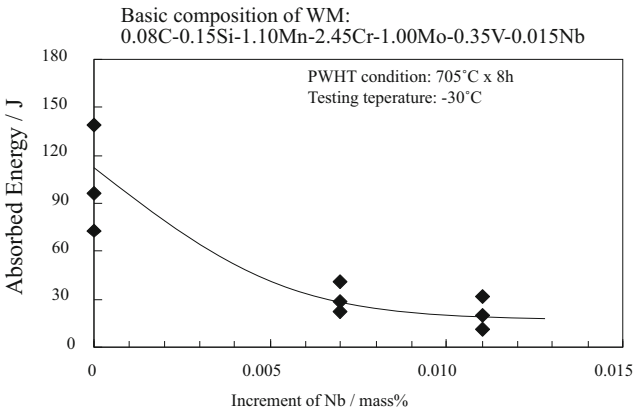

Fig. 9 Relationship between increase of Nb and impact toughness of $2^1/_4$Cr-1Mo-V steel SAW metal

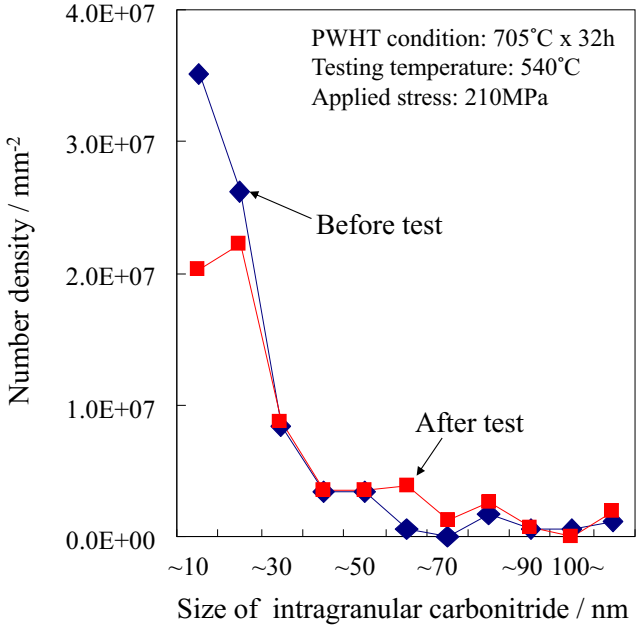

Fig. 10 Change of carbonitride size distribution around the creep rupture test of $2^1/_4$Cr-1Mo-V SAW metal

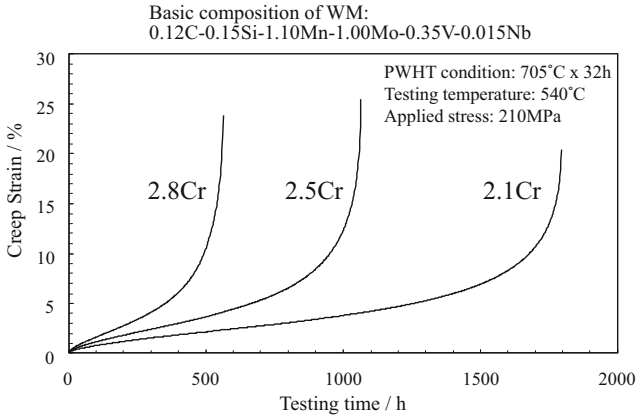

Fig. 12 Creep curves of Cr-controlled $2^1/_4$Cr-1Mo-V SAW metal

where vTr55 signifies 55-J transition temperature. Figure 5 shows schematic for defining ΔvTr55.

The Vickers hardness of deposited metal was also measured. The measurement position was at the cross section of the test plate and the center of the deposited metal and 1/2 t position of test plate.

2.4 Microstructure evaluation of weld metal

The morphology of the precipitates in deposited metal was observed by means of transmission electron microscope (TEM, Hitachi/H-8000). Three-dimensional atom probe (3D-AP, CAMECA/LEAP 3000HR) was also used to observe this as well as the impurities in the prior γ grain boundary. Each position of observation was located at as-casted zone of the final pass at which the microstructure could be clearly observed without any disturbance due to heat affection by the upper weld pass.

3 Results and discussion

3.1 Test results and a discussion about creep rupture property of $2^1/_4$Cr-1Mo-V steel weld metal

It is important to evaluate the creep deformation of $2^1/_4$Cr-1Mo-V steel weld metal in order to understand a valid way to improve its creep rupture property.

Generally, the creep rate of material at elevated temperatures depends on temperature (T) and stress (σ) and can be described as Eq. 1 [9]. Also, the creep deformation of material can be identified according to stress component (n) in Eq. 1, as shown in Table 6.

Fig. 11 Relationship between Cr content and the amount of solute Nb and V atom in the matrix calculated by Thermo-Calc. (version S/data base TCFE_6)

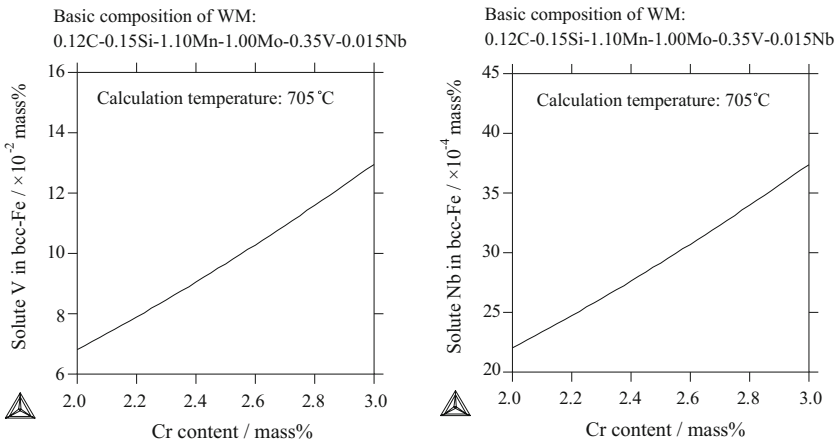

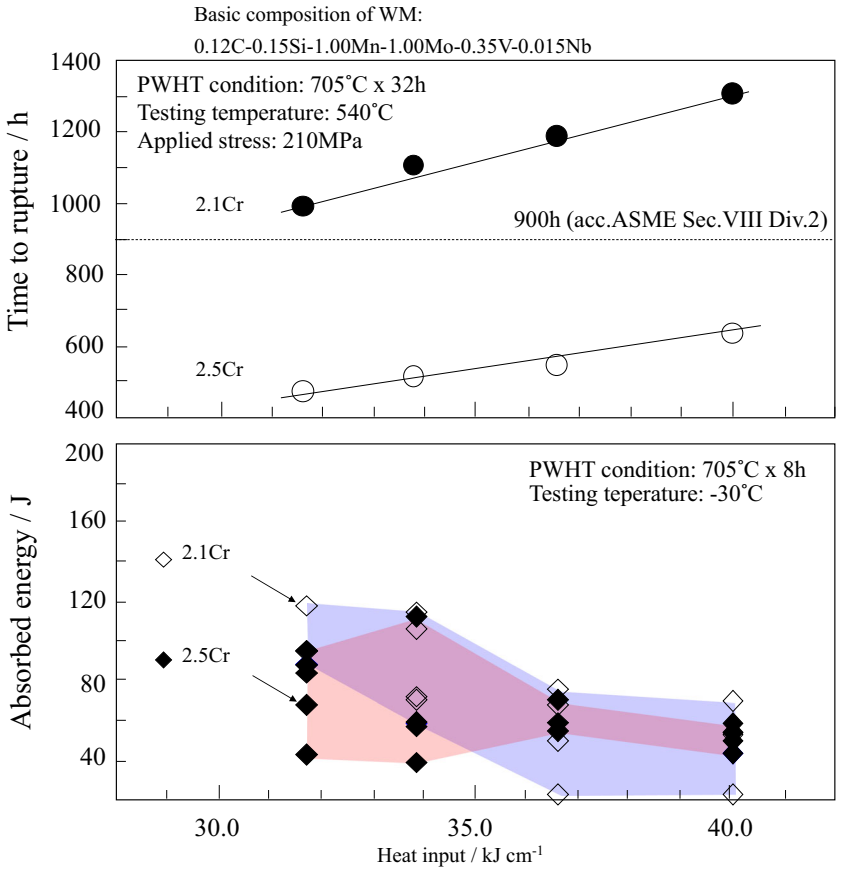

Fig. 13 Comparison of the creep rupture property of two-Cr-level of $2^1/_4$Cr-1Mo-V steel SAW metal under various heat input conditions

$$\dot{\varepsilon} = \varepsilon_o \frac{G\Omega}{k_b T}\left(\frac{b}{d_g}\right)^p \left(\frac{\sigma}{G}\right)^n \frac{D}{b^2} \quad (1)$$

where

ε	creep rate
ε_o	material constant
G	Young's modulus
Ω	atomic volume
k_b	Boltzman constant
p	grain size exponent
b	burger's vector
d_g	grain size
n	stress exponent
D	effective diffusion coefficient

Equation 1 can be described as Eq. 2 when the temperature (T) is constant.

$$\log \dot{\varepsilon} = C + n\log\sigma \quad (2)$$

where

C constant

From this point of view, creep rupture tests of $2^1/_4$Cr-1Mo-V steel SAW metal with typical chemical composition, refer to Table 3, were conducted under several applied stresses in

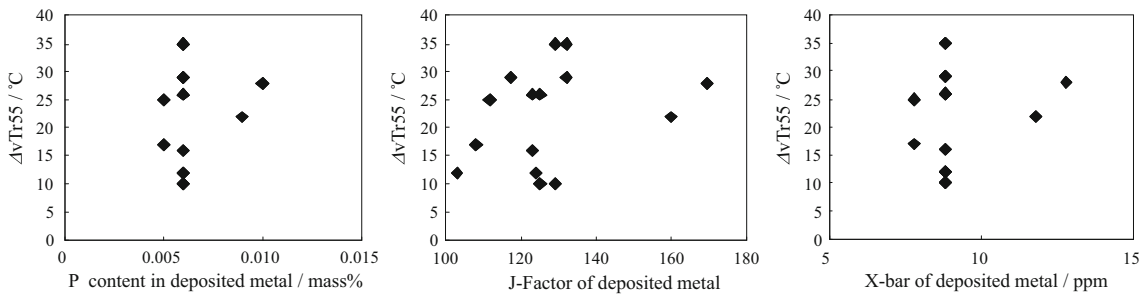

Fig. 14 Relationship between P, J-Factor, X-bar, and ΔvTr55

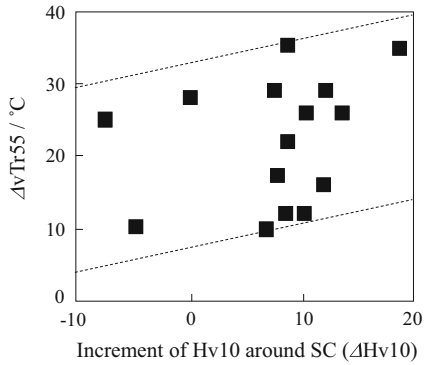

Fig. 15 Relationship between ΔHv10 and ΔvTr55

order to evaluate stress components (n). The testing temperature was 540 °C. Figure 6 shows the relationship between applied stress and creep rate at 540 °C, where there was a linear relationship between the two on a double logarithmic plot as described in Eq. 2. Its gradient is equal to the stress component (n) and found to be approximately 9. This result indicates that the creep deformation of the steel weld metal is dislocation creep according to Table 6. Therefore, it assumed that the increase in number density of MX-type precipitate inhibits the annihilation of dislocation which improves the creep rupture property of deposited metal.

The increase in Nb content increases the creep rupture property of the deposited metal as shown in Fig. 7. Figure 8 shows bright field images of these Nb containing weld deposits. The change in size and shape is evident from these images. Therefore, the design of MX-type precipitate for this weld metal can improve the creep rupture properties.

On the other hand, the Nb increase of deposited metal could also degrade its impact toughness. Figure 9 shows the relationship between Nb increase and the impact toughness of $2^1/_4$Cr-1Mo-V steel SAW metal. The impact toughness of deposited metal was degraded because of Nb increase.

It is assumed that increase in Nb and V contents remarkably increases the volume faction of MX and improves the creep strength of deposited metal, though degrading its impact toughness. Therefore, the creep rupture property of $2^1/_4$Cr-1Mo-V steel weld metal should be improved not by the increase of Nb or V but the change in other alloying elements.

It is obvious that the amount of MX is an important factor for the creep rupture property of $2^1/_4$Cr-1Mo-V steel weld metal. However, the thermo-dynamical stability of MX must be also important. Figure 10 shows the change of the carbonitride size distribution around the creep rupture test of $2^1/_4$Cr-1Mo-V SAW metal. Finer carbonitride decreased whereas the coarser ones increased during the test. This result indicates that MX grow under high temperature over a long period of time.

The theoretical equation of the Ostwald growth of M_aX_b-type carbonitride is described as Eq. 3 [10].

$$r^3 = r_0^3 + \frac{8}{9}\left(\frac{a+b}{a}\right)\frac{\sigma D_M V^\theta u_M}{RT\left(u_M^\theta - u_M\right)^2}t \tag{3}$$

where

r	particle size of carbonitride
r_0	initial particle size of carbonitride
a, b	valance of M_aX_b (a=b=1, when MX is considered)
σ	interfacial energy between the matrix and carbonitride
D_M	diffusion coefficient of solute atom in the matrix
V^θ	volume fraction of precipitation per mol of solute atom
u_M	solute atom density in the matrix
u^θ_M	solute atom density in carbonitride
t	holding time

According to Eq. 3, particle size of MX depends on u_M when holding time is constant, because all factors except for u_M are particular values for the material. This indicates that the decrease of the solute Nb and V atom density in the matrix could inhibit the Ostwald growth of MX and will improve the creep rupture property of $2^1/_4$Cr-1Mo-V steel weld metal.

From the view point of the above, the amount of change of the solute Nb and V atom in the matrix by various alloying elements is calculated by Thermo-Calc. (version S/data base TCFE_6). Figure 11 shows the relationship between Cr content and the amount of solute Nb and V atom in the matrix. The calculation temperature was 705 °C, which was the typical PWHT temperature for $2^1/_4$Cr-1Mo-V steel weld metal. The calculated result indicates that the decrease of Cr content reduces the amount of the solute Nb and V atom in the matrix.

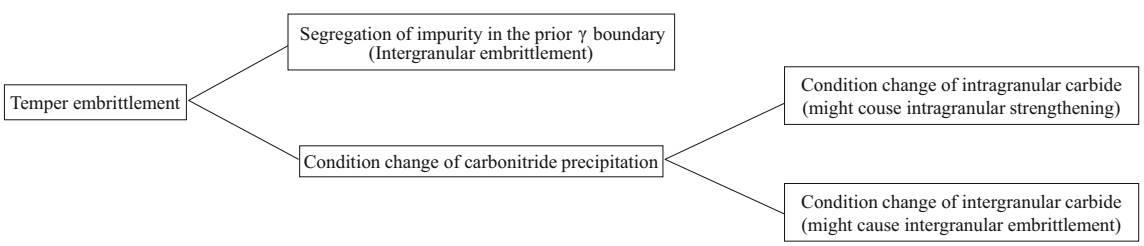

Fig. 16 Typical TEM images of $2^1/_4$Cr-1Mo-V SMAW metal during step cooling

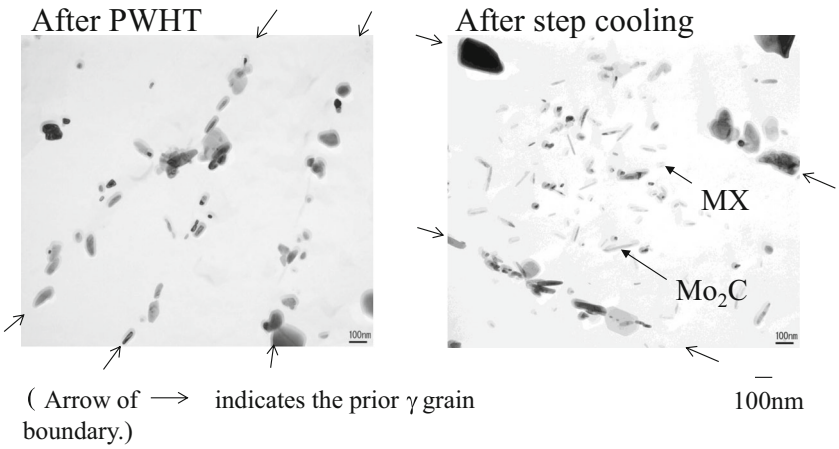

Fig. 17 Schematic of main mechanism of Cr-Mo steel's temper embrittlement

The creep rupture tests of $2^1/_4$Cr-1Mo-V steel SAW metal with three levels of Cr content were conducted. The Cr content of deposited metal was controlled as 2.1, 2.5, and 2.8 mass%. As shown in Fig. 12, the creep rupture property of $2^1/_4$Cr-1Mo-V steel SAW metal was improved as its Cr content decreased. Especially, as shown in Fig. 13, SAW metal of 2.1 mass%Cr shows greater creep rupture property than that of 2.5 mass%Cr and satisfied the regulation of ASME code

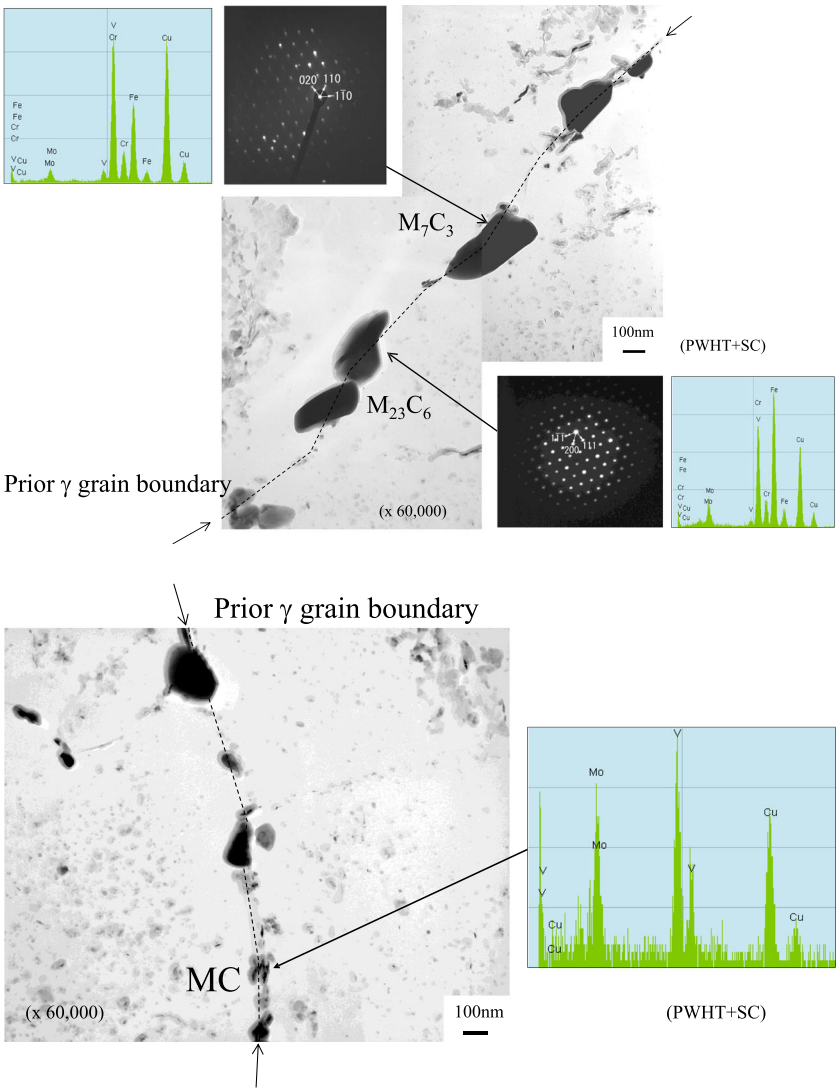

Fig. 18 Typical TEM images around a prior γ grain boundary of $2^1/_4$Cr-1Mo-V steel SMAW metal

under various heat input conditions. Figure 13 also shows impact toughness of each material. From the figure, it is evident that creep rupture life can be increased, without significantly degrading the toughness, by decreasing the Cr content.

This improvement in creep rupture property is due to the decrease in Nb and V contents in the matrix with the reduced Cr content resulting in decrease in Ostwald coarsening of the MX-type precipitates during creep testing. This fine MX-type precipitates pin the dislocation movement. Therefore, creep property of this weld metal can be improved by reducing the Cr content as it reduces the size of the MX-type precipitates.

3.2 Test results and a discussion about temper embrittlement property of $2^1/_4$Cr-1Mo-V steel weld metal

The temper embrittlement of Cr-Mo steel generally results from intergranular embrittlement, and it is widely known that the segregation of impurities to the prior γ grain boundary causes it. Figure 14 shows the relationships between P, J-Factor, X-bar, and ΔvTr55 of $2^1/_4$Cr-1Mo-V SMAW metal. There seems to be a great dispersion of data, so the mutuality between these was not obvious.

When ΔHv10 is defined as the change of the Vickers hardness of deposited metal during step cooling, ΔHv10 and ΔvTr55 have a linear relationship with each other as shown in Fig. 15.

Here, the hardening of $2^1/_4$Cr-1Mo-V deposited metal during step cooling occurs, resulting from the precipitation of fine carbonitrides such as MX and Mo_2C, as shown in Fig. 16. This relationship between ΔHv10 and ΔvTr55 indicates that relative intergranular embrittlement occurs by the hardening of the crystal grain during step cooling. However, there is also a great dispersion of data. The factor of temper embrittlement of $2^1/_4$Cr-1Mo-V SMAW metal is considered to fall into several categories as shown in Fig. 17 but could not be marshalled not only by intergranular embrittlement from impurity segregation or intragranular strengthening from carbonitride precipitation. Therefore, the effect of intergranular carbonitride to temper embrittlement should also be considered.

Figure 18 shows typical TEM images around a prior γ grain boundary of $2^1/_4$Cr-1Mo-V SMAW metal. Coarse carbide such as M_7C_3 and $M_{23}C_6$ and fine carbide such as MC were observed here. Evaluation was focused on the effect of these carbides on intergranular embrittlement.

The relationship between the amount of change of the coarse carbide in the prior γ grain boundary around step cooling (ΔN) and ΔvTr55 was evaluated. Test materials of which C, Cr, V, and Nb content were controlled in order to change the distributed state of the intergranular carbide were prepared. When carbide, of which the circle-equivalent diameter was over 0.5 μm in the prior γ grain boundary, was defined as coarse, ΔvTr55 increased as ΔN increased, as shown in Fig. 19, which also indicates that the material design of high

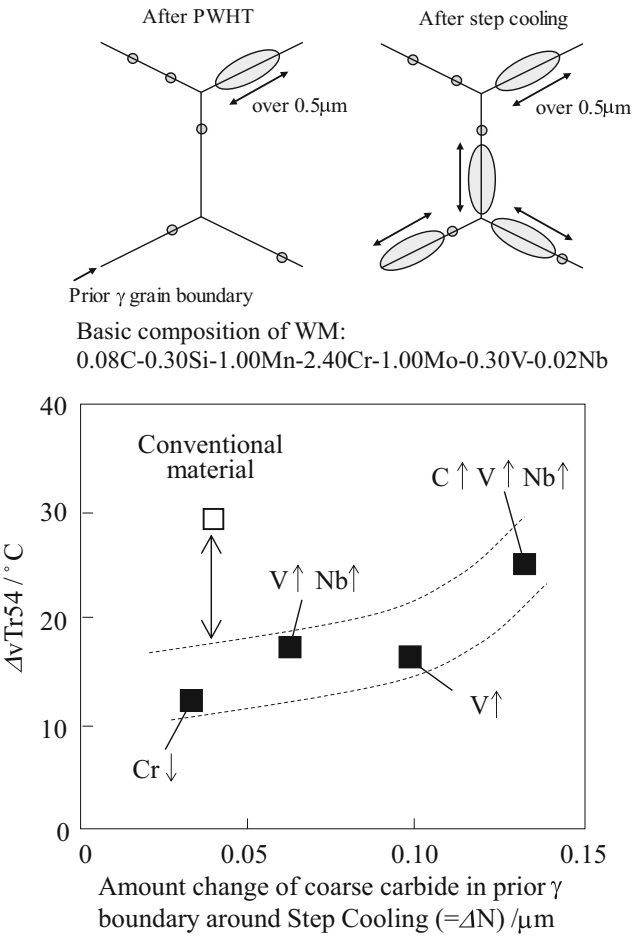

Fig. 19 Relationship between ΔN and ΔvTr55 of $2^1/_4$Cr-1Mo-V steel SMAW metal

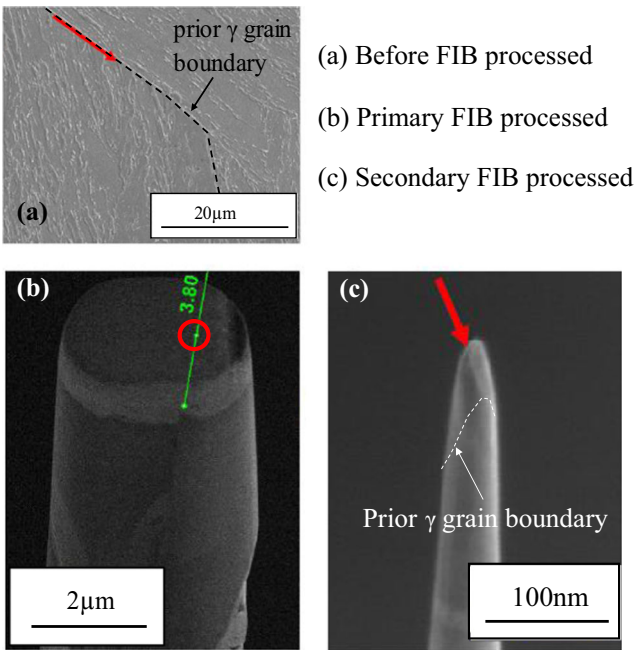

Fig. 20 FIB processing schematic for 3D-AP observation specimen of $2^1/_4$Cr-1Mo-V steel SMAW metal

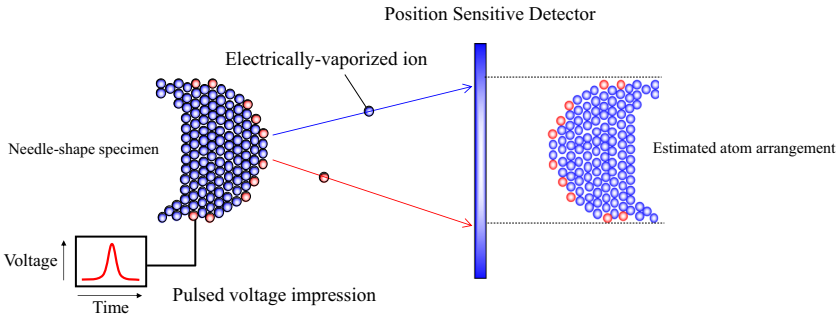

Fig. 21 Schematic of 3D-AP observation principle

MC and low $M_7C_3/M_{23}C_6$ content with lower Cr and higher C, V, and Nb content has less temper embrittlement sensitivity compared to conventional material. This suggests that intergranular carbide together with impurities in the prior γ grain boundary has some kind of interaction with each other.

After this, the existence forms of carbide and impurities in the prior γ grain boundary were evaluated by 3D-AP in order to clarify their interaction. The concept of 3D-AP observation is shown below. A minute needle-shape specimen, which contained the prior γ grain boundary, was removed from $2^1/_4$Cr-1Mo-V steel SMAW metal by focused ion beam (FIB) machining method, as shown in Fig. 20.

Figure 21 shows the schematic of the 3D-AP observation principle. When pulsed voltage was energized in this needle-shape specimen, ionized atoms flew from the specimen surface to a position sensitive detector. Also, an atom arrangement which composed the needle-shape specimen was estimated by energized voltage, pulse fraction, and flight time of each atom.

Figure 22 shows the 3D-AP observation result of $2^1/_4$Cr-1Mo-V steel SMAW metal. Concentrations of Cr and V atom were observed in the prior γ grain boundary and were verified as M_7C_3 and MC by atomic ratio analyzing, respectively. On the other hand, concentrations of P atoms were observed in the prior γ grain boundary. P segregation in prior γ grain boundary which might cause intergranular embrittlement was visually captured by 3D-AP. In addition, concentrations of P atoms were also observed at the interface between M_7C_3 and the matrix, as well as inside MC. The schematic of this result is described in Fig. 23.

After this, the atomic profiles of Cr, V, and P were analyzed around these carbides in the prior γ grain boundary. Figure 24 shows the atomic profiles by 3D-AP, analyzing M_7C_3 and MC in the prior γ grain boundary of $2^1/_4$Cr-1Mo-V steel SMAW metal. This result also indicates that P segregates at the interface between M_7C_3 and the matrix, while P exists in VC. In

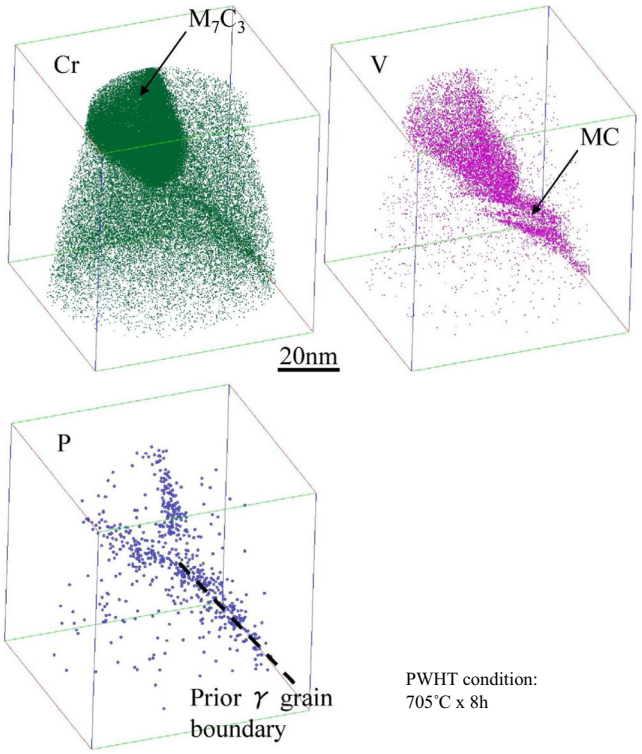

Fig. 22 Atom arrangement around prior γ grain boundary of $2^1/_4$Cr-1Mo-V SMAW metal verified by 3D-AP

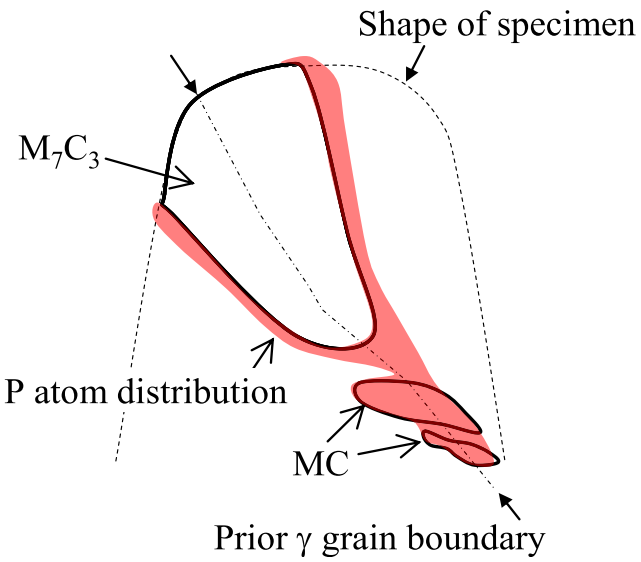

Fig. 23 Schematic of 3D-AP observation result of $2^1/_4$Cr-1Mo-V steel SMAW metal

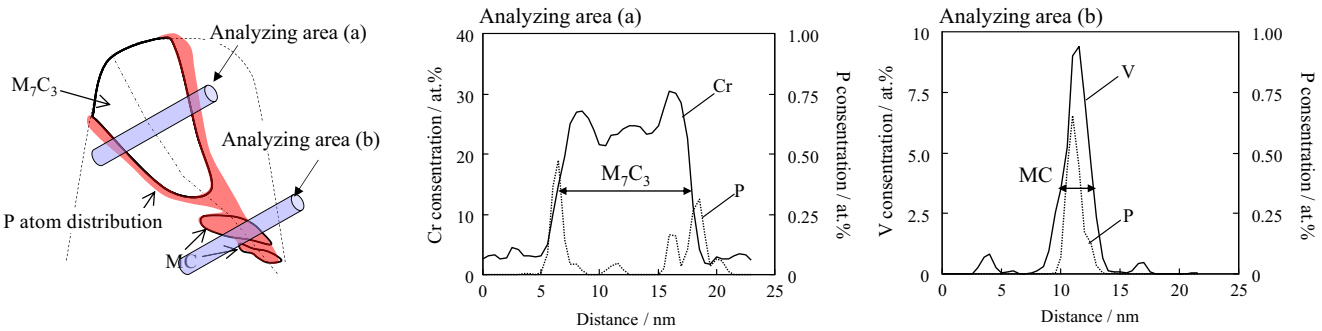

Fig. 24 Atomic profile around M_7C_3 and MC in the prior γ grain boundary of $2^1/_4$Cr-1Mo-V steel SMAW metal by 3D-AP analyzing

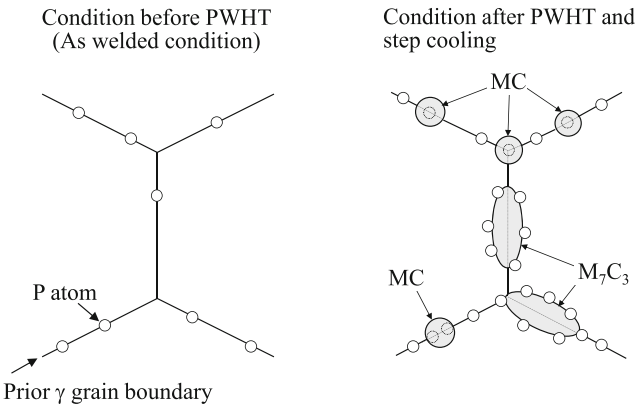

Fig. 25 Schematic of condition change in the prior γ grain boundary of $2^1/_4$Cr-1Mo-V steel weld metal during PWHT and step cooling

other words, it is considered that M_7C_3 does not dissolve P in its crystal structure while MC does.

These results, mentioned above, are explained below. Figure 25 shows the schematic of the conditional changes in the prior γ grain boundary of $2^1/_4$Cr-1Mo-V steel weld metal during PWHT and step cooling. Both coarse carbides (M_7C_3) and fine carbides (MC) precipitate in the prior γ grain boundary during PWHT process. While intergranular embrittlement is caused by the segregation of impurities such as P, MC cancels out the effect of P by dissolving it in its crystal structure. However, M_7C_3 does not dissolve P like MC does. P segregates in the prior γ grain boundary and the interface between M_7C_3 and the matrix. Therefore, intergranular embrittlement is promoted according to the increase of the embrittlement area. Therefore, material design with high MC but low M_7C_3 content could be valid for $2^1/_4$Cr-1Mo-V steel weld metal in order to reduce temper embrittlement sensitivity. According to the calculations by Thermo-Calc, the decrease of Cr and the increase of V are considered to be valid to achieve this, as shown in Fig. 26.

SMAW metal with lower Cr and higher V content in order to decrease M_7C_3 and increase MC was tested in addition to conventional SMAW metal. As shown in Fig. 27, the insoluble Cr content, producing M_7C_3-type chemical compound in deposited metal, decreased while the insoluble V content, producing MC-type chemical compound in deposited metal, increased, due to the Cr decrease and the V increase in the deposited metal. Figure 28 shows the relationship between ΔvTr55 and vTr55+3ΔvTr55 of conventional and developed $2^1/_4$Cr-1Mo-V steel SMAW metal. Here, vTr55+3ΔvTr55 is one index for judging temper embrittlement property as referred to in API RP A934-A. ΔvTr55 was lowered because of the decrease of Cr and the increase of V, and its vTr55+3ΔvTr55 was also of quite a low value.

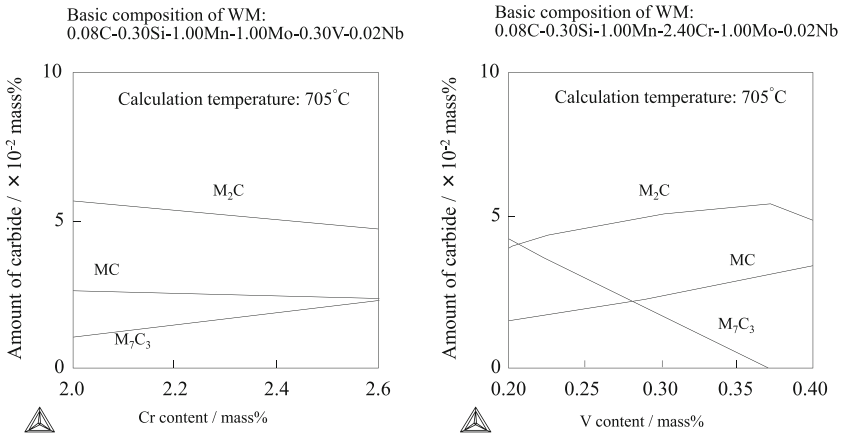

Fig. 26 Relationship between Cr and V content and the amount of carbide calculated by Thermo-Calc. (version S/data base TCFE_6)

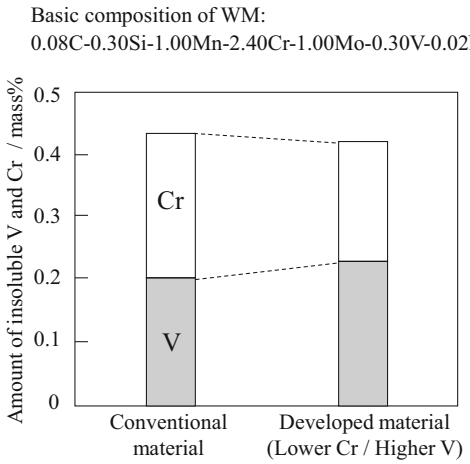

Fig. 27 Comparison of the amount of soluble V and Cr in conventional and developed $2^1/_4$Cr-1Mo-V steel SMAW metal

4 Conclusion

The validity of intergranular and intragranular precipitates to creep rupture and temper embrittlement properties of $2^1/_4$Cr-1Mo-V steel weld metal were discussed.

Creep deformation of $2^1/_4$Cr-1Mo-V steel weld metal was determined as dislocation creep. Application of fine carbonitrides such as MX was valid for improving the creep rupture property of $2^1/_4$Cr-1Mo-V steel weld metal by inhibiting the annihilation dislocation under elevated temperatures. Especially, the decrease of Cr content slows down the Ostwald growth of MX and improves the creep rupture property of $2^1/_4$Cr-1Mo-V steel weld metal without degrading impact toughness very much.

The temper embrittlement of $2^1/_4$Cr-1Mo-V steel weld metal resulted from intergranular embrittlement was promoted by the increase of coarse carbides such as M_7C_3 in the prior γ grain boundary. The P segregation, which causes intergranular embrittlement, was visually identified in the prior γ grain boundary and the interface between M_7C_3 and the matrix by 3D-AP, while P existed inside MC. It is considered that the increase of M_7C_3 expands the embrittlement area and promotes intergranular embrittlement, whereas MC cancels out the effect of P by dissolving it in its crystal structure. As a result, $2^1/_4$Cr-1Mo-V steel weld metal with lower Cr and higher V contents, showed a superior property against temper embrittlement compared to conventional material.

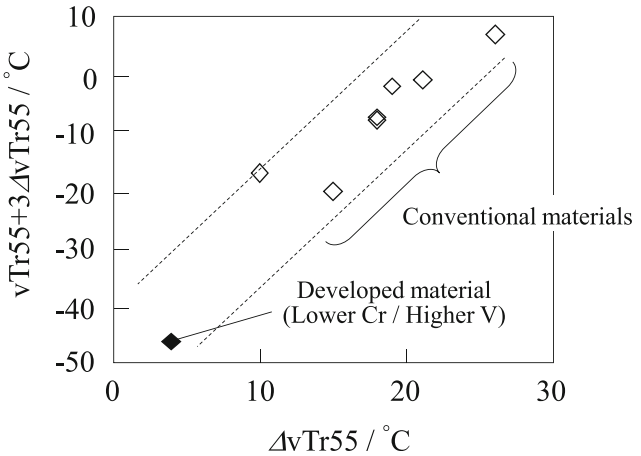

Fig. 28 Relationship between ΔvTr55 and vTr55+3ΔvTr55 of conventional and developed $2^1/_4$Cr-1Mo-V steel SMAW metal

References

1. Nose S et al (2000) Big strides to a world leading heavy wall pressure vessel manufacturer. Kobe steel engineering reports 50:3
2. Nose S et al. (1998) Fitness-for-service evaluations in petroleum and fossil power plants (ASME). PVP 380
3. American Society of Mechanical Engineer (2009) Section VIII, Division 2
4. American Petroleum Institute (2008) Recommended practice, 934-A, 2nd edn
5. Bruscato R (1970) Temper embrittlement and creep embrittlement in 2-1/4 Cr-1 Mo shielded metal arc weld deposits. Weld J 49:148s–156s
6. Watanabe J et al. (1978) Japan steel works technical report. 38:69–78
7. Nakata H et al (2002) Grain boundary phosphorus segregation under thermal aging in low alloy steels. INSS J 9:171
8. Guttmann M et al (1982) The thermodynamics of interactive co-segregation of phosphorus and alloying elements in iron and temper-brittle steels. Metall Trans A 13A:1693
9. Maruyama K et al (1997) Material science of strength at elevated temperature. Journal of Materials Science 37(16):15–24
10. Wei MY et al (1980) Growth of alloy carbide particles in austenite. Tetsu to Hagane 66:S1178